

Complex Wavelet Transform for Analog Signal Processing

Sandro A. P. Haddad[†], Joel M. H. Karel[‡], Ralf L. M. Peeters[‡],
Ronald L. Westra[‡] and Wouter A. Serdijn[†]

[†]Electronics Research Laboratory, Faculty of Electrical Engineering, Mathematics and Computer Science,
Delft University of Technology, Mekelweg 4, 2628 CD Delft, The Netherlands
Email: [s.haddad, w.a.serdijn]@ewi.tudelft.nl

[‡]Department of Mathematics, University of Maastricht P.O.Box 616, 6200 MD, Maastricht, The Netherlands
Email: [joel.karel,Ralf.Peeters,Westra]@math.unimaas.nl

Abstract—This paper presents an analog implementation of the complex wavelet transform using both the complex first order system (CFOS) and the Padé approximation. The complex wavelet filter design is based on the combination of the real and the imaginary state-space descriptions that implement the respective transfer functions. In other words, a complex filter is implemented by an ordinary state-space structure for the real part and an extra C matrix for the imaginary part. Several complex wavelets, such as Gabor, Gaussian and Morlet complex wavelets, are obtained and simulations demonstrate excellent approximations to the ideal wavelets.

I. INTRODUCTION

Complex wavelets provide more detail information in transient signal detection than real-valued wavelets. Often the wavelet transform of a real signal with complex wavelet is plotted in modulus-phase form, rather than real and imaginary representation. In the complex wavelet transform analysis, the modulus maxima and the phase crossings point out the locations of sharp signal transitions. Nevertheless, the phase information reveals isolated singularities in a signal more accurately than does the modulus [1]. Also, using the phase information, different kinds of transition points of the analyzed signal, i.e. local maxima and inflection points, can be distinguished. For instance, using the first complex Gaussian wavelet (*cgau1*), the $-\pi$ to $+\pi$ phase crossings point define the inflection points, whereas $\pm\pi$ to 0 is associated with the local maxima points (peaks), as one can see in Fig.1.

Section II treats the complex wavelet bases and deals with the computation of a transfer function which describes a certain wavelet base that can be implemented as an analog filter. Section III describes the circuit designs. Some results provided by simulations are given in Section IV. Finally, Section V presents the conclusions.

II. COMPLEX WAVELET FILTERS

A. Complex wavelet bases

One example of complex wavelet function is the Gabor wavelet. The Gabor wavelet is obtained from a complex Gaussian function (complex sinusoids windowed by a Gaussian

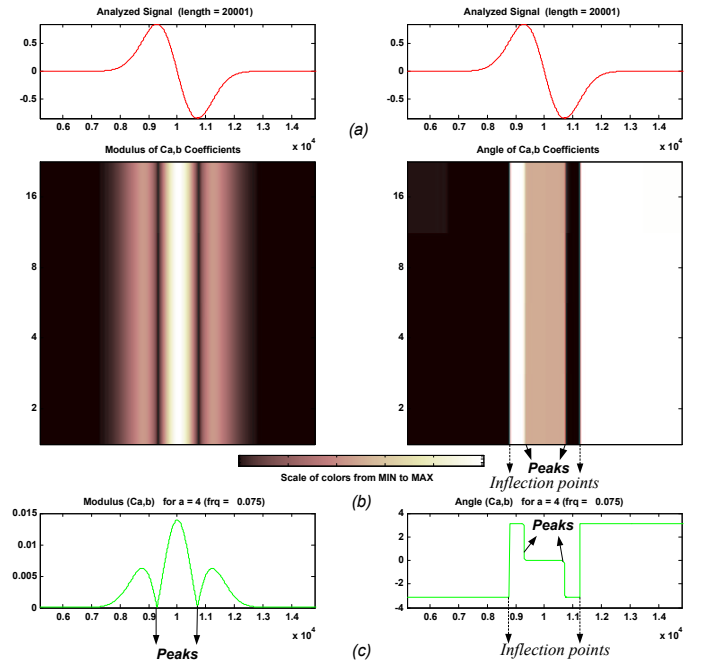


Fig. 1. Complex wavelet transform using *cgau1* (a) Input signal (b) Wavelet transform coefficients with four dyadic ($a = 2^i$) scales (c) One coefficient line ($a = 2^2 = 4$)

function) as basic functions, as described by

$$\psi(t) = C \cdot e^{-j\omega t} e^{-t^2} = C \cos(\omega t) e^{-t^2} - j C \sin(\omega t) e^{-t^2} \quad (1)$$

where $e^{-j\omega t} e^{-t^2}$ is the complex Gaussian function and C is a normalizing constant. From the Gabor wavelet one can derive some complex wavelet families, e.g. the complex Gaussian and the complex Morlet. The complex Morlet is obtained by simply apply $\omega = \pi \sqrt{\frac{2}{\ln 2}} \simeq 5.3364$ [2] in Eq.1.

The complex Gaussian wavelet family is defined from the derivatives of the Gabor wavelet and is given by

$$\psi(t) = C \cdot \frac{d^n}{dt^n} (e^{-j\omega t} e^{-t^2}) \quad (2)$$

where n denotes n -th derivative, $\frac{d}{dt}$ is the symbolic derivative and C is a normalized constant.

The wavelet used in this paper is the complex Gabor wavelet, from which we can derive other complex wavelets. The modulus, the real and imaginary parts and the phase of the complex Gabor wavelet for $\omega = 2$ are given in Fig.2.

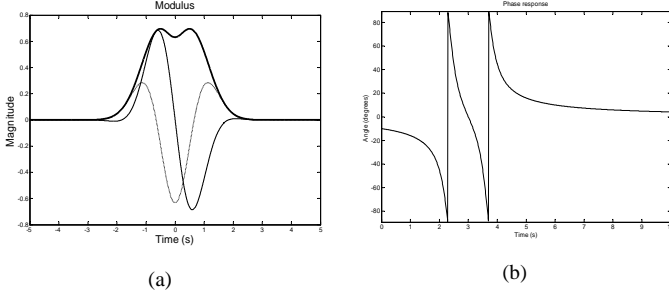


Fig. 2. Complex Gabor Wavelet (a) Modulus (b) Phase

B. Complex First Order filters

In order to implement the complex Gabor wavelet filter, we first propose an analog filter based on Complex First Order Systems (CFOS) [3]. A CFOS is defined by the following set of equations

$$\dot{x}(t) = (\sigma + j\omega)x(t) + (c_{re} + jc_{imag})u(t) \quad (3)$$

$$x(t) = x_{re}(t) + jx_{imag}(t) \quad (4)$$

where u is an input signal assumed to be real, x is a state variable assumed to be complex, σ , ω , c_r and c_i are system parameters assumed also to be real. One can map this first order transfer function onto a state space description. The general expression of the transfer function corresponding to a state space description is

$$H(s) = C \cdot (sI - A)^{-1} \cdot B + D \quad (5)$$

The entries of the matrices A , B , C and D are derived directly from the coefficients of the transfer function. The poles of the transfer function are the eigenvalues of A . In other words, the denominator of the transfer function is given by the determinant of $sI - A$, where I is the identity matrix. The zeros of the filter are constituted from the contents of all four system matrices. Considering $D = 0$, and applying $C \cdot adj(sI - A) \cdot B$, where adj compute the adjoint of the respective matrix, we can obtain a possible state space description of H_{re} and H_{imag} given by

$$\begin{aligned} A_{re,im} &= \begin{bmatrix} -\sigma & \omega \\ -\omega & \sigma \end{bmatrix} & B_{re,im} &= \begin{bmatrix} 0 \\ 1 \end{bmatrix} \\ C_{re} &= \begin{bmatrix} 0 & 1 \end{bmatrix} & C_{im} &= \begin{bmatrix} 1 & 0 \end{bmatrix} \end{aligned} \quad (6)$$

Notice that the state space descriptions differentiate only by the C matrices. Then, we can represent the CFOS using the following block diagram, given in Fig.3

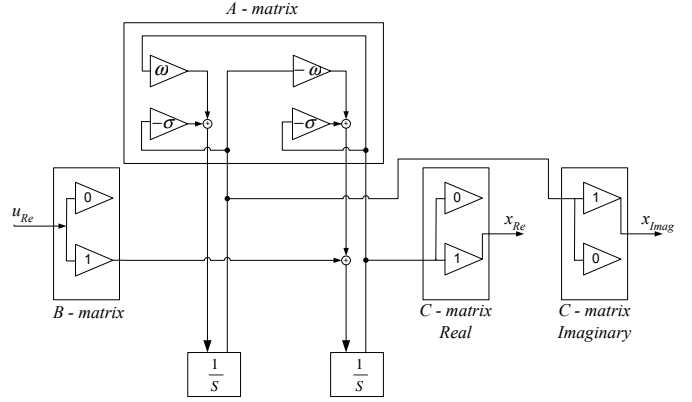


Fig. 3. Complex First Order System block diagram using state-space representation

The imaginary input can be added by just including another B stage. From this block diagram, one can easily derive the common CFOS cross-coupled representation in Fig.4

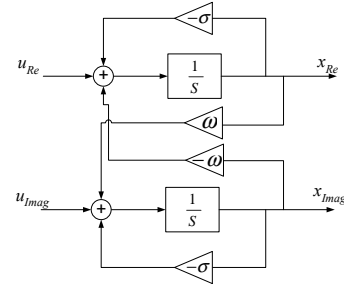


Fig. 4. Complex First Order System block diagram

The starting point of the Gabor wavelet design using CFOS is the definition of the number of stages which defines the appropriate Gaussian envelope to set the width of the wavelet [3].

Subsequently, once the Gaussian envelope has been defined, the real and the imaginary impulse responses are obtained. Applying Eq. 3 and Eq. 4, the complex impulse response of $n + 1$ CFOS stages is given by

$$h(t) = (c_{re} + jc_{imag})^{n+1} \frac{t^n}{n!} e^{(\sigma+j\omega)t} U_{-1}(t) \quad (7)$$

From Eq.7 one easily calculates the general transfer function of the $n + 1$ CFOS system for the real and the imaginary outputs, which are given as follows

$$H_{re}(n) = \frac{(s + \sigma) \cdot H_{re}(n-1) - \omega \cdot H_{imag}(n-1)}{((s + \sigma)^2 + \omega^2)^n} \quad (8)$$

$$H_{imag}(n) = \frac{(s + \sigma) \cdot H_{imag}(n-1) + \omega \cdot H_{re}(n-1)}{((s + \sigma)^2 + \omega^2)^n} \quad (9)$$

with

$$H_{re}(1) = \frac{(s + \sigma)}{(s + \sigma)^2 + \omega^2} \quad (10)$$

$$H_{imag}(1) = \frac{\omega}{(s + \sigma)^2 + \omega^2} \quad (11)$$

which correspond to the transfer function of the first order complex filter in Fig.3.

Choosing the right values for σ and ω , we can obtain the imaginary and the real part of the complex Gabor, respectively, as one can see in Fig.5 for different numbers of stages.

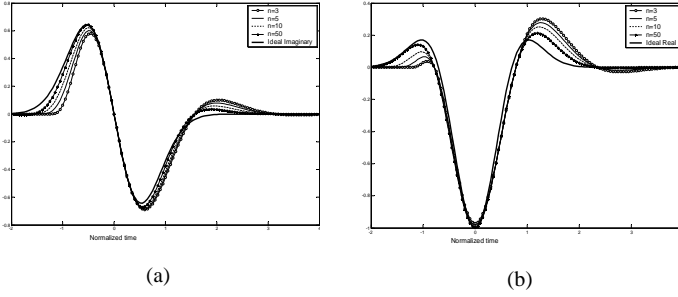


Fig. 5. Complex Gabor Impulse response (a) Imaginary output (b) Real output

It must be noted that the Complex Morlet Wavelet can also be approximated in a similar manner. Likewise, we need to choose the right value for ω in order to have the appropriate frequency component for the Morlet wavelet.

C. Padé Approximation using Taylor expansion

In the previous section, an analog complex wavelet transform filter was proposed, of which the impulse responses are approximated Gaussian window functions. This complex wavelet filter, subsequently, was implemented with Complex First Order Systems (CFOS). However, a more general procedure based on the Padé approximant to obtain various types of wavelet bases was presented in [4]. Moreover, the Padé method proves to be more successful than the method using CFOS for a filter of the same order which will be shown in this section.

Just like the Taylor expression, the Padé approximation is an approximation that concentrates around one point of the function that needs to be approximated (i.e. the impulse response $h(t)$) [5]. In the Padé approximation, the coefficients of the approximating rational expression are computed from the Taylor coefficients in the Laplace domain of the original function. The reason to apply the Padé approximation to the Laplace transform of $h(t)$ is, that it immediately yields a rational expression which is suitable for implementation. A Padé approximation of function $F(s)$ is given by

$$\hat{F}(s) = \frac{P(s)}{Q(s)} = \frac{p_0 + p_1s + \dots + p_m s^m}{q_0 + q_1s + \dots + q_n s^n} \quad (12)$$

where $\hat{F}(s)$ is the Taylor series truncated around some point, e.g. $s = 0$. If the approximation rational function has a numerator of order m and a denominator of order n , the original function can be approximated up to order $m+n$. The computation of the coefficients of $P(s)$ and $Q(s)$ has already been described in [4].

Therefore, one can first apply the Padé function to approximate the Gaussian envelope. We apply a [2/5] Padé approximation, i.e. $m = 2$ and $n = 5$, which yields an approximation of order $k = 7$ of the Taylor series expansion. The transfer function resulting from this approximation is given by

$$H_{gaus}(s) = \frac{5.7s^2 - 18.2s + 92.416}{s^5 + 8.3s^4 + 33s^3 + 74.8s^2 + 94.5s + 52.3} \quad (13)$$

In order to obtain the transfer function of the real and the imaginary parts of the Gabor function in Eq.1 one can easily apply

$$H_{Gabor}(s) = \frac{s}{s^2 + \omega^2} * H_{gaus}(s) + j \frac{\omega}{s^2 + \omega^2} * H_{gaus}(s) \quad (14)$$

where the asterisk $*$ is the symbol for convolution and $\frac{s}{s^2 + \omega^2}$ and $\frac{\omega}{s^2 + \omega^2}$ are the Laplace functions of $\cos(\omega t)$ and $\sin(\omega t)$, respectively. Notice that both transfer functions are related by

$$H_{Real}(s) = \frac{s}{\omega} * H_{Imag}(s) \quad (15)$$

From Eq.15, one can verify that the poles of the real and the imaginary transfer function are the same, only differentiating in the zeros. Therefore, we can implement both transfer functions by changing only the C-matrix of the state-space representation, as shown in Fig.6.

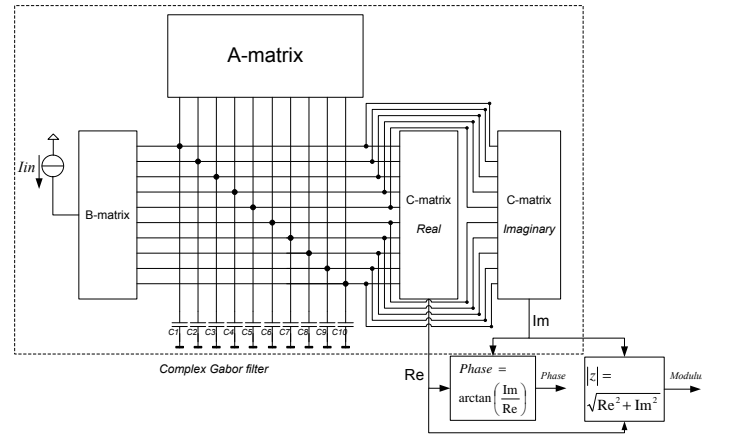


Fig. 6. Block diagram of the Complex Wavelet system

Using the procedure described in Eq.14, yields in tenth order transfer functions and the corresponding impulse responses are given in Fig.7.

In order to compare the Padé approximation with the approximation using CFOS one can verify the associated Mean-Square Error for both approximation. The results obtained

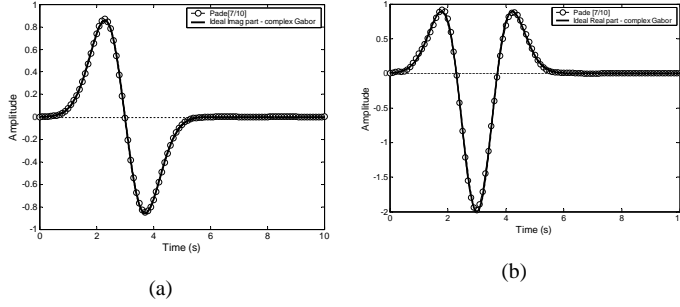


Fig. 7. Complex Gabor Impulse response approximation using Padé [7/10] (a) Imaginary output (b) Real output

varying the order of the filter are illustrated in Table.I, where the real and the imaginary parts of the complex Gabor wavelet have been approximated, respectively.

order	CFOS		Padé	
	Real	Imaginary	Real	Imaginary
3	0.0444	0.0513	0.0899	0.0927
4	0.0382	0.0380	0.0817	0.0468
5	0.0339	0.0302	0.0454	0.0185
6	0.0308	0.0251	0.0178	6.05e-3
7	0.0284	0.0216	7.75e-3	1.01e-3
8	0.0265	0.0190	2.30e-3	0.040e-3
9	0.0250	0.0170	0.74e-3	0.033e-3
10	0.0238	0.0154	0.13e-3	0.020e-3

TABLE I

ORDER OF THE FILTER VERSUS MEAN-SQUARE ERROR FOR CFOS AND PADÉ APPROXIMATION

As seen from the Mean-Square Error comparison, the Padé method yields a much better approximation than the method using CFOS for a filter of the same order.

Finally, by only changing the numerator coefficients of the previous transfer function (i.e. the zeros), we can obtain the complex Gaussian and the complex Morlet wavelets.

III. CIRCUIT DESIGN

A. Filter design

The filter design that follows is based on an orthonormal ladder structure [6], which presents a good behavior with respect to sensitivity and dynamic range [4], with log-domain integrators as the main building blocks. A simple bipolar multiple-input low-power log-domain integrator [7] will be used as the basic building block for the implementation of the state space equation of the Gabor wavelet filter described in the previous section. This log-domain integrator is shown in Fig.8.

B. Modulus stage

The static translinear principle can be applied to the implementation of the functions of the following stages. First,

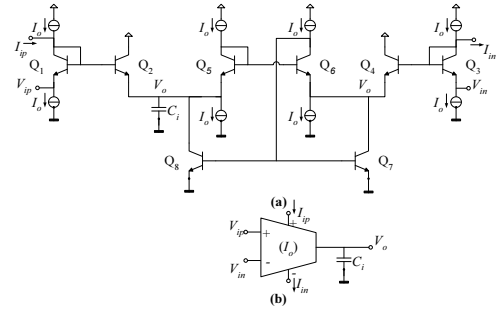


Fig. 8. (a) The multiple-input low power log-domain integrator, and (b) its symbol [7]

the required modulus function $|z| = \sqrt{\text{Re}^2 + \text{Im}^2}$ is realized with the circuit in Fig.9 [8]. The translinear loops in the circuit consist of transistors Q_1, Q_7, Q_8 and Q_4 and Q_6, Q_{11}, Q_{10} and Q_4 , implementing

$$\begin{aligned} 2(I_o - \text{Re})(I_o + \text{Re}) &= (\sqrt{2}I_o - z)(\sqrt{2}I_o + z) \\ 2(I_o - \text{Im})(I_o + \text{Im}) &= (\sqrt{2}I_o - z)(\sqrt{2}I_o + z) \end{aligned} \quad (16)$$

where I_o is the bias current. Notice that both variables, Re and Im, are bipolar quantities.

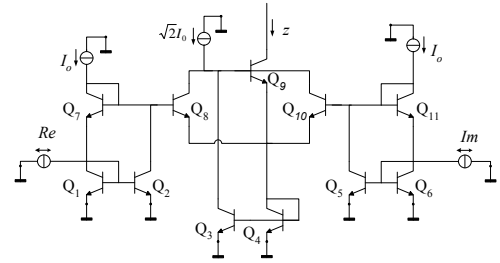


Fig. 9. Modulus (Vector magnitude) circuit [8]

C. Phase information - Arctangent stage

From the complex waveforms shown in Fig.7, we can now obtain the phase information by simply applying the arctangent to the ratio between the imaginary and the real outputs. This operation can be approximated using the translinear principle as [8]

$$\text{Phase} = \frac{\text{Im}}{0.63\text{Re} + \sqrt{0.88\text{Re}^2 + \text{Im}^2}} \simeq \frac{2}{\pi} \arctan\left(\frac{\text{Im}}{\text{Re}}\right) \quad (17)$$

where the square root term is provided by the modulus circuit in previous section. The division operation can easily be implemented using the factorization $z = \frac{x}{y} \Rightarrow \frac{I_o+z}{I_o-z} = \frac{y+x}{y-x}$ [8] and the schematic is given in Fig.10 [9].

IV. SIMULATIONS RESULTS

To validate the circuit principle, we have simulated the filter, the modulus stage and the phase stage using models of IBM's 0.18 μm BiCMOS IC technology. The filter has

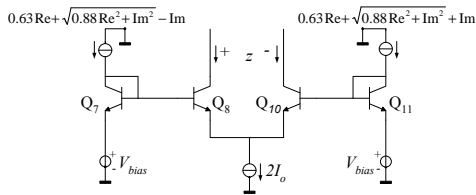


Fig. 10. Divider circuit for the Arc tangent stage [9]

been designed to operate from a 1.2V supply and a 100pF total capacitance. Fig.11 shows the impulse response of the real and imaginary outputs of the wavelet filter. The excellent approximation of the complex Gabor wavelet can be compared with the ideal Gabor function to confirm the performance of the filter. Finally, Fig.12 shows the modulus stage and phase stage outputs, which are close to the ideal cases for the complex Gabor wavelet.

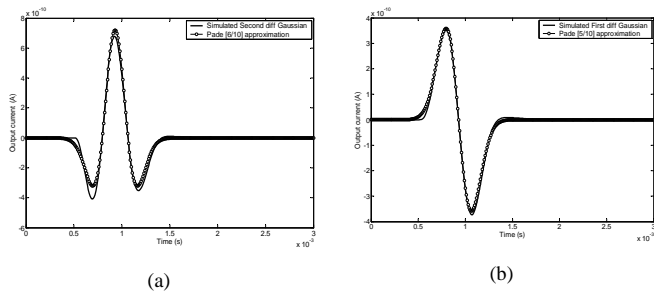


Fig. 11. Simulated impulse responses of the complex Gabor wavelet filter (a) Imaginary output (b) Real output

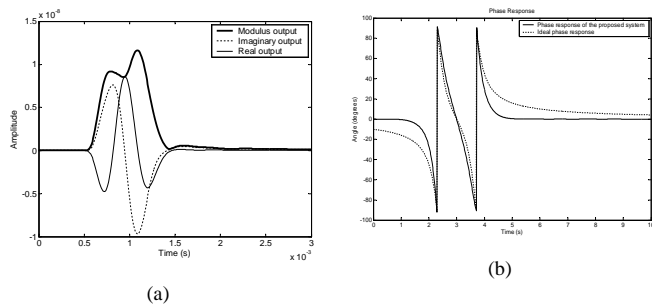


Fig. 12. Simulated complex Gabor wavelet filter (a) Modulus responses and (b) Phase response

V. CONCLUSIONS

An analog implementation of the complex wavelet transform was presented. The procedure was based on the CFOS and the Padé approximation approaches. The complex wavelet filter design was derived from the combination of the real and the imaginary state-space descriptions. By this, we were able to implement a complex filter, i.e. both real and imaginary

transfer functions, with just an extra C matrix into an ordinary state-space structure. Several complex wavelets have been obtained and simulations demonstrated excellent approximations to the ideal wavelets.

REFERENCES

- [1] M. Unser and A. Aldroubi, "A review of wavelets in biomedical applications," *Proceeding of the IEEE*, vol. 84, no. 4, April 1996.
- [2] I. Daubechies, *Ten Lectures on Wavelets*, Society for Industrial and Applied Mathematics, Philadelphia, 1992.
- [3] H. Kamada and N. Aoshima, "Analog gabor transform filter with complex first order system," in *Proc. SICE*, pp. 925–930, 1997.
- [4] S. A. P. Haddad, S. Bagga, and W. A. Serdijn, "Log-domain wavelet bases," in *Proceedings IEEE International Symposium Circuits and Systems*, May 2004, vol. 1, pp. 1100–3.
- [5] G. A. Baker Jr., *Essentials of Pade Approximants*, Academic Press, New York, 1975.
- [6] D. A. Johns, W. M. Snelgrove, and A. S. Sedra, "Orthonormal ladder filters," *IEEE Transactions on Circuits and Systems*, vol. 36, no. 3, pp. 337–343, March 1989.
- [7] M. N. El-Gamal and G. W. Roberts, "A 1.2v npn-only integrator for log-domain filtering," *IEEE Transactions on Circuits and Systems - II: Analog and Digital Signal Processing*, vol. 49, no. 4, pp. 257–265, April 2002.
- [8] E. Seevinck, *Analysis and Synthesis of Translinear Integrated Circuits*, Elsevier, The Netherlands, 1988.
- [9] C. Toumazou, F. J. Lidgley, and D. G. Haigh, *Analogue IC design: the current-mode approach*, IEE circuits and systems series 2, United Kingdom, 1990.